Scripta Materialia 150 (2018) 61–65

Contents lists available at ScienceDirect

Scripta Materialia

journal homepage: www.elsevier.com/locate/scriptamat

Regular article

Influence of pre-implanted helium on dislocation loop type in tungsten under self-ion irradiation

R.W. Harrison *, J.A. Hinks, S.E. Donnelly

School of Computing and Engineering, University of Huddersfield, Queensgate, Huddersfield HD1 3DH, UK

ARTICLE INFO

Article history:
Received 19 December 2017
Received in revised form 6 February 2018
Accepted 25 February 2018
Available online xxxx

Keywords:
Tungsten
Irradiation
Fusion
Dislocation
In situ TEM

ABSTRACT

Transmission electron microscopy with in-situ ion irradiation has been used to examine dislocation loop formation during self-ion irradiation of pristine W and samples pre-implanted with He. Dislocation loops with $\boldsymbol{b} = \pm\frac{1}{2}\langle 111\rangle$ and $\boldsymbol{b} = \langle 100\rangle$ were observed in both the pristine W and samples pre-implanted with He. This contrasts previous works with He/H ion irradiation where no $\boldsymbol{b} = \langle 100\rangle$ type loops have been observed in W. The $\boldsymbol{b} = \langle 100\rangle$ dislocation loops form during the cascade and He has no effect on the type of dislocation loop formed; unlike $\boldsymbol{b} = \langle 100\rangle$ type loop nucleation in FeCr alloys.

Tungsten (W) is the leading candidate for use as the divertor armour in the International Thermonuclear Experimental Reactor (ITER) and the Demonstration (DEMO) fusion reactor [1]. The divertor armour is a plasma facing component (PFC) and thus will experience high heat fluxes and displacement damage from 14.1 MeV neutrons and He ion bombardment. These particles will impact on the W surface resulting in a profile of He concentration throughout the structure. In our previous work [2,3] using He ion irradiation, the dislocation loop population in W is dominated by $\boldsymbol{b} = \frac{1}{2}\langle 111\rangle$ type with no $\boldsymbol{b} = \langle 001\rangle$ being observed. Matsui et al. [4] also reported the formation of dislocation loops with $\boldsymbol{b} = \pm\frac{1}{2}\langle 111\rangle$ type in only W and Mo samples irradiated with 10 keV D ions at room temperature to fluences of 3×10^{18} ions/cm^2. A similar result has also been observed in H ion irradiation of Ta-W alloys where dislocation loops were found to be of $\boldsymbol{b} = \frac{1}{2}\langle 111\rangle$ type [5] at doses up to 1.55 DPA at an irradiation temperature of 350 °C. However, Fengfeng et al. [6] reported the formation of $\boldsymbol{b} = \langle 001\rangle$ type loops in W irradiated with 20 keV He ions to a dose of 5×10^{15} ions/cm^2 at 800 °C.

Eyre and Bullough [7] reported that two types of interstitial loops were present in irradiated body-centred cubic (BCC) Fe alloys: $\boldsymbol{b} = \frac{1}{2}\langle 111\rangle$ and $\boldsymbol{b} = \langle 001\rangle$. They concluded that the nucleus was a faulted interstitial-type dislocation loop on {110} planes containing a stacking fault which could be removed by shear produced from the partial dislocation reactions shown in Eqs. (1) and (2) [7];

$$\frac{1}{2}[110] + \frac{1}{2}\left[00\bar{1}\right] = \frac{1}{2}\left[11\bar{1}\right] \tag{1}$$

$$\frac{1}{2}[110] + \frac{1}{2}\left[\bar{1}10\right] = [010] \tag{2}$$

The $\frac{1}{2}\langle 111\rangle$ split interstitial in W has been reported to be more favourable than the $\frac{1}{2}\langle 110\rangle$ and $\langle 100\rangle$ with formation energies of 9.55, 9.84 and 11.49 eV, respectively [8,9], and the unfaulting of a $\frac{1}{2}\langle 110\rangle$ loop via Eq. (2) would be highly unlikely and has been shown to have a probability of 1 in 10^{19} in Mo at room temperature [10]. Jäger and Wikens [11] observed the formation of faulted $\boldsymbol{b} = \pm\frac{1}{2}\langle 110\rangle$ loops in W with 60 keV Au ions which would shear at a critical size of ~0.9–2.0 nm. However, Jäger and Wikens [11] observed an overall dominance for $\boldsymbol{b} = \frac{1}{2}\langle 111\rangle$ type agreeing with the very low probability of a faulted loop shearing via Eq. (2).

This trend for the damage microstructure to be dominated by $\boldsymbol{b} = \pm\frac{1}{2}\langle 111\rangle$ loops in the presence of He has been observed previously in FeCr alloys by Prokhodtseva et al. [12]. The authors [12] noted a shift in the type of Burgers vectors of the dislocation loop population from a dominance of $\boldsymbol{b} = \langle 100\rangle$ type in single beam Fe ion irradiations to a dominance of $\boldsymbol{b} = \pm\frac{1}{2}\langle 111\rangle$ loops in the simultaneous Fe and He ion

* Corresponding author.
E-mail address: r.w.harrison@hud.ac.uk (R.W. Harrison).

https://doi.org/10.1016/j.scriptamat.2018.02.040

irradiations. It has been theorised that the $\boldsymbol{b} = \langle 100 \rangle$ loop arises from interaction and reaction of two $\boldsymbol{b} = \pm\frac{1}{2}\langle 111 \rangle$ loops in BCC materials [13,14] as shown in Eq. (3) (from Ref. [14]).

$$\frac{1}{2}[111] + \frac{1}{2}\left[\overline{1}\overline{1}1\right] = [001] \tag{3}$$

Thus for the FeCr alloys, Prokhodtseva et al. [12] proposed that in the presence of He, the mobility of the $\boldsymbol{b} = \frac{1}{2}\langle 111 \rangle$ type loops is low leading to less chance of interaction and coalescence with another $\boldsymbol{b} = \frac{1}{2}\langle 111 \rangle$ type loop that would lead to loops with $\boldsymbol{b} = \langle 100 \rangle$. Xu et al. [13] have used atomistic kinetic Monte Carlo (kMC) simulations to also show that the formation of $\langle 100 \rangle$ loops occurs directly from atomistic interaction between two $\boldsymbol{b} = \frac{1}{2}\langle 111 \rangle$ loops in Fe. However, in more recent work, Schäublin et al. [15] reported that Cr content increases the likelihood of formation of $\langle 100 \rangle$ type loops in FeCr alloys at low dose (0.05 DPA) where $\boldsymbol{b} = \frac{1}{2}\langle 111 \rangle$ loop interaction is unlikely and may arise from Cr presence in the damage after the thermal spike of the cascade.

It has been reported that the formation of energetically less favourable $\boldsymbol{b} = \langle 100 \rangle$ dislocation loops occurs almost exclusively in Fe alloys [13] whereas $\boldsymbol{b} = \pm\frac{1}{2}\langle 111 \rangle$ dislocation loops dominate for W [4] and Mo [16]. However, Yi et al. [17,18] irradiated W samples with 150 keV W ions to a total of 3 DPA at an irradiation temperature up to 800 °C. The authors observed small (~5 nm) dislocation loops mainly with $\boldsymbol{b} = \pm\frac{1}{2}\langle 111 \rangle$ [17]. However, around 25% were found to be of $\boldsymbol{b} = \langle 100 \rangle$ type. Yi et al. [18] found the fraction of $\boldsymbol{b} = \langle 100 \rangle$ type loops decreased with increasing irradiation temperature and almost no $\langle 100 \rangle$ loops were observed at 800 °C. This was attributed to the free energies of $\boldsymbol{b} = \langle 100 \rangle$ loops increasing more rapidly compared to $\boldsymbol{b} = \pm\frac{1}{2}\langle 111 \rangle$ types as the loops grow in size showing there is a temperature consideration (as well as the material considerations discussed above) in the formation of $\boldsymbol{b} = \langle 100 \rangle$ type loops in W. Sand et al. [19] have performed molecular dynamics (MD) simulations on the impact of a 150 keV W primary knock-on atom (PKA) and found that the formation of $\boldsymbol{b} = \langle 100 \rangle$ loops occurred as a direct result of the cascade collapse, agreeing well with the work of Yi et al. [17,18].

In this work we studied the effect of self-ion irradiation on the dislocation type(s) observed in pristine and He-implanted W samples, using sequential transmission electron microscopy (TEM) with in-situ ion irradiation under conditions matching our previous work [2,3]. This has allowed us to examine the effect of He and cascade size on the formation of $\boldsymbol{b} = \langle 100 \rangle$ dislocation loops in W.

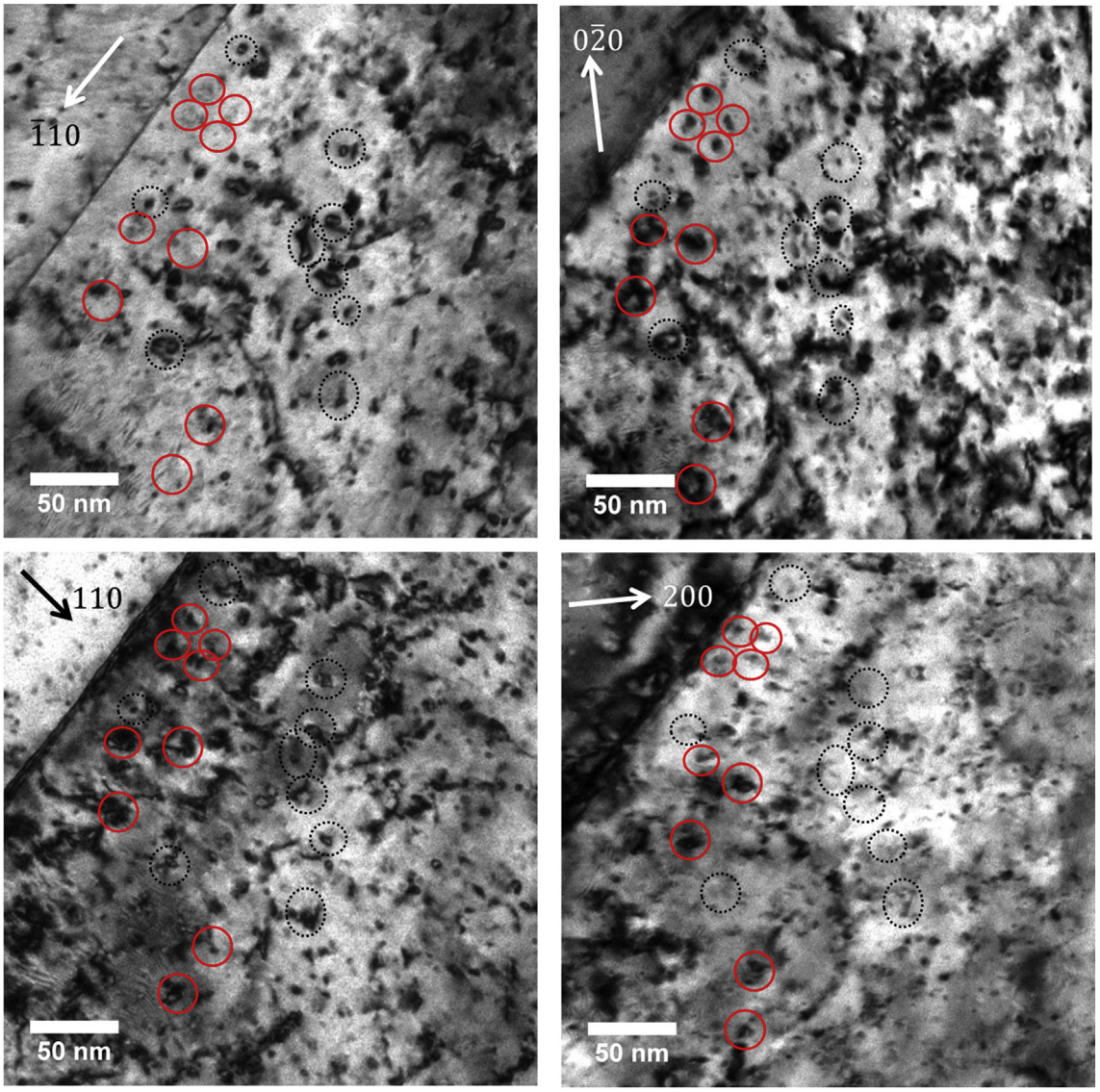

Fig. 1. Two-beam TEM images of a W sample irradiated with W ions to a dose of 3.0 DPA at 500 °C taken with a) $\boldsymbol{g} = (\bar{1}10)$, b) $\boldsymbol{g} = (0\bar{2}0)$, c) $\boldsymbol{g} = (110)$ and d) $\boldsymbol{g} = (200)$. The dislocation loops circled with dashed lines are $\boldsymbol{b} = \langle 100 \rangle$ type loops and solid lines are $\boldsymbol{b} = \pm\frac{1}{2}\langle 111 \rangle$ loops.

Samples for TEM were produced from W foil (Alfa-Aesar, 99.95 wt%) by electropolishing which has been described elsewhere [2]. Pre-screening of the samples showed no presence of dislocation loops when imaged under two-beam conditions using $\boldsymbol{g}$ vectors in the [001] and [113] zone axes. In-situ ion irradiation was performed at the Microscopes and Ion Accelerators for Materials Investigations facility (MIAMI) utilising the MIAMI-2 system. MIAMI-2 consists of a 350 kV ion accelerator coupled with a Hitachi H-9500 TEM (operated at 200 kV) in which the ion beam is incident at 18.7° to the electron beam. Samples were pre-implanted with He using 10 keV He^+ ions at room temperature to a concentration of 1500 atomic parts per million (appm) of He (~9×10^{14} ions/cm^2). The pre-implanted and pristine W samples were then irradiated using 350 keV W^+ ions at 500 °C to a dose of 3.0 DPA (achieving a He-appm/DPA ratio of 500 for the He implanted samples, to match our previous work [2,3]). The flux of W ions was ~3×10^{13} ions/cm^2/s and samples were irradiated to a total fluence of ~1×10^{15} ions/cm^2. The *Stopping Range of Ions in Matter* (SRIM-2013) Monte Carlo code [20] was used to calculate DPA and He concentration due to implantation using the method of DPA calculation proposed by Stoller et al. [21]. Burgers vectors of the dislocation loops were determined using the $\boldsymbol{g}.\boldsymbol{b} = 0$ criterion with analysis of ~50–60 loops per sample. Post-irradiation examination was also performed with a JEOL JEM-3010 TEM operated at 200 kV. Weak-beam dark-field (WBDF) imaging was performed under ($\boldsymbol{g}$,3$\boldsymbol{g}$) conditions for $\boldsymbol{g} = (0\bar{2}0)$. Dislocation loop sizes were measured from the WBDF micrographs taking the major diameter of the loop core.

Fig. 1a–d show a pristine W sample irradiated to 3.0 DPA at 500 °C. The dislocation loops circled with dashed lines are loops that are present when $\boldsymbol{g} = (110)$ and $(\bar{1}10)$ and show invisibility when $\boldsymbol{g} = (200)$ or $(0\bar{2}0)$ corresponding to $\boldsymbol{b} = [010]$ or [100], respectively. Dislocation loops circled with solid lines in Fig. 1a–d are loops with either $\boldsymbol{b} = \pm\frac{1}{2}[\bar{1}11]$, $\pm\frac{1}{2}[1\bar{1}1]$ or $\pm\frac{1}{2}[111]$. This shows that $\boldsymbol{b} = \langle 100\rangle$ type dislocation loops do form under self-ion irradiation in pristine W in good agreement with previous experimental work [17] and MD simulations [19]. The percentage of $\boldsymbol{b} = \langle 100\rangle$ loops observed in these samples was between 35 and 40%.

Fig. 2a–d show a W sample pre-implanted with He to a concentration of 1500 appm and subsequently irradiated to 3.0 DPA with W ions at 500 °C. The dislocation loops circled with dashed lines indicate loops that are observable when $\boldsymbol{g} = (110)$ and $(\bar{1}10)$ and show invisibility when $\boldsymbol{g} = (200)$ or $(0\bar{2}0)$ corresponding to $\boldsymbol{b} = [010]$ or [100], respectively. Dislocation loops circled with solid lines in Fig. 2a–d indicate loops that are $\boldsymbol{b} = \pm\frac{1}{2}\langle 111\rangle$ type. The percentage of $\boldsymbol{b} =$

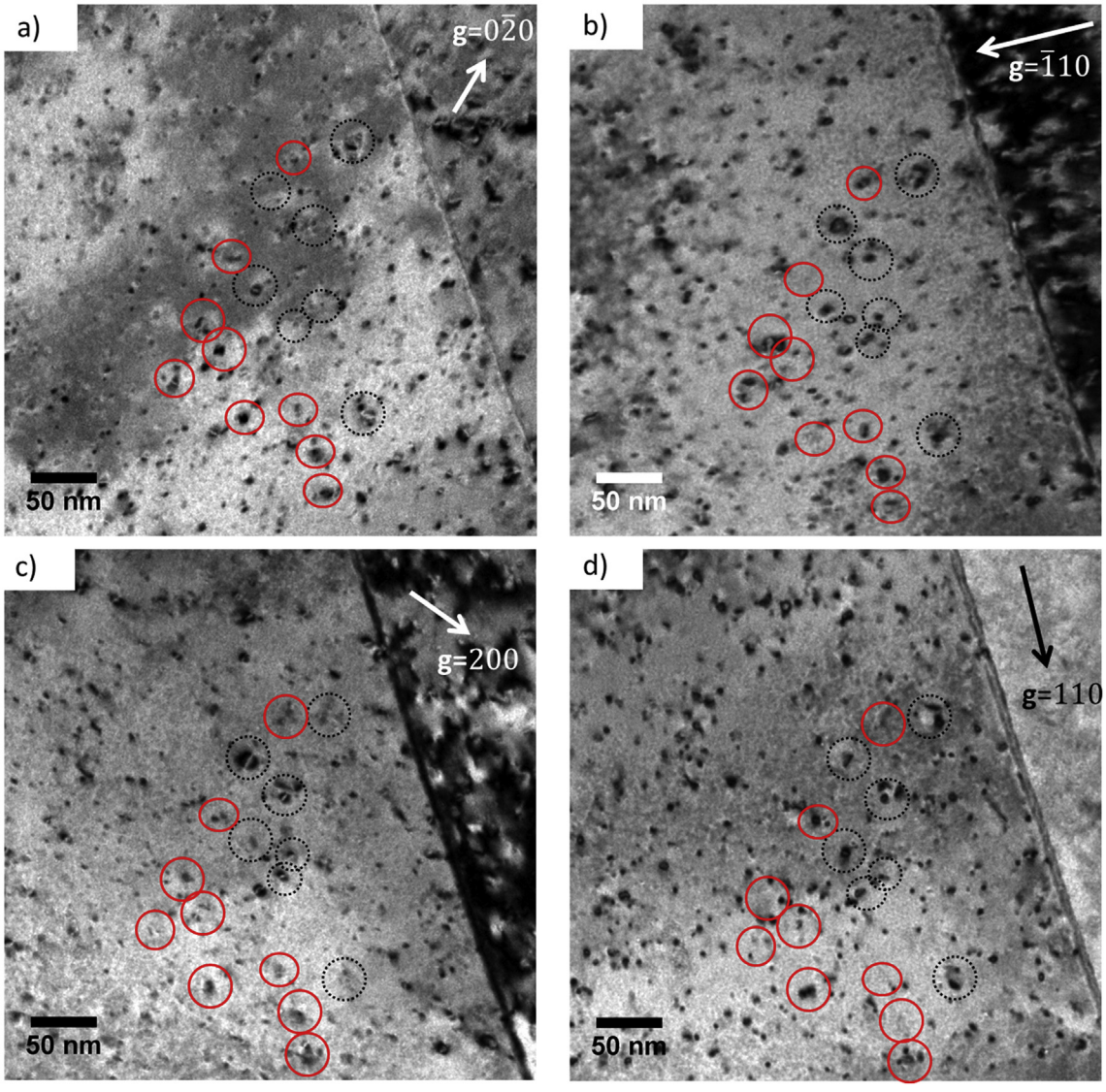

Fig. 2. Two-beam TEM images of W sample pre-implanted with He to 1500 appm He and then irradiated with W ions to a dose of 3.0 DPA at 500 °C taken with a) $\boldsymbol{g} = (0\bar{2}0)$, b) $\boldsymbol{g} = (\bar{1}10)$, c) $\boldsymbol{g} = (200)$ and d) $\boldsymbol{g} = (110)$. The dislocation loops circled with dashed lines are $\boldsymbol{b} = \langle 100\rangle$ type loops and solid lines are $\boldsymbol{b} = \pm\frac{1}{2}\langle 111\rangle$ loops.

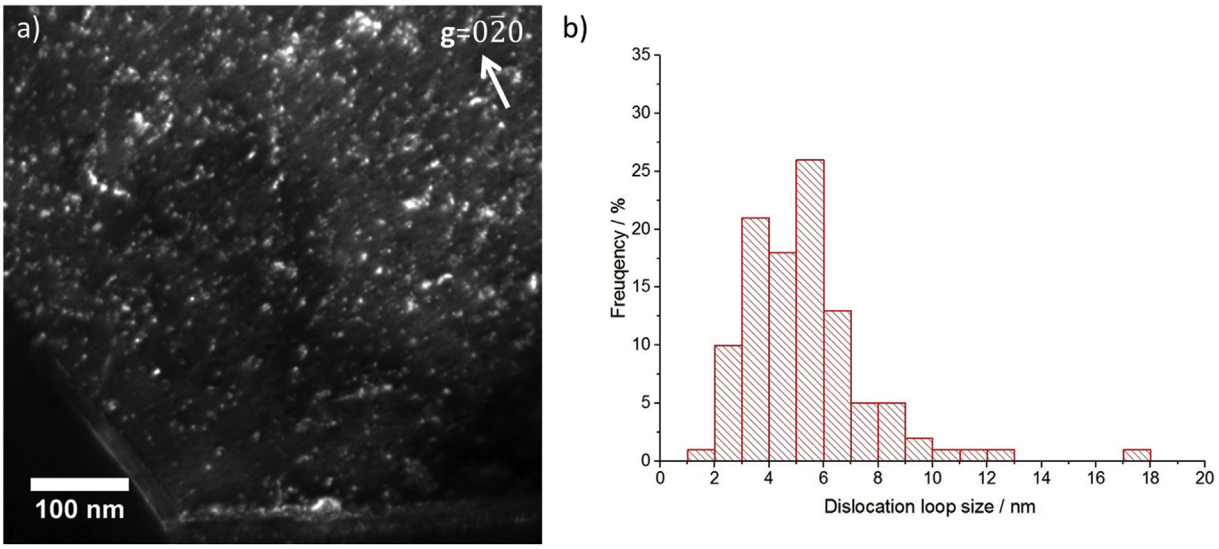

Fig. 3. a) WBDF image of self-ion irradiated pristine W sample irradiated to a dose of 3.0 DPA at a temperature of 500 °C under (***g***,3***g***) conditions where $\boldsymbol{g} = (0\bar{2}0)$ and b) a histogram of dislocation loop sizes measured under these conditions.

⟨100⟩ loops observed in the pre-implanted He samples was similar to the pristine W samples (~35–40%). Pre-implantation of He seems to have no effect on the formation of $\boldsymbol{b} = \langle 100 \rangle$ loops contrary to results reported for Fe alloys [12,13]. This is also contrary to our previous work [2,3] where we irradiated W with 15, 60 or 85 keV He ions to a total of 3.0 DPA at temperatures between 500 and 1000 °C observing loops only with $\boldsymbol{b} = \pm\frac{1}{2}\langle 111 \rangle$. Under He [2,3], H [5] or D [4] ion irradiation there will be widely-spaced dilute cascades formed with many isolated Frenkel pairs [22] resulting in a low average energy density. This work shows that the lack of $\boldsymbol{b} = \langle 100 \rangle$ type loops in previous light ion irradiations (i.e. He [2,3], H [5] or D [4]) was not due to the presence of impurity gas atoms inhibiting migration and reaction of $\boldsymbol{b} = \pm\frac{1}{2}\langle 111 \rangle$ loops but rather to the absence of dense cascade damage in good agreement with predictions from MD simulations [19].

Recent characterisation of neutron irradiated W has predominantly focused on dislocation loop, voids and precipitate size with no characterisation of dislocation type being performed [23–27]. Rau [28] annealed fast-neutron irradiated ($E > 1$ MeV) W to a temperature of 1100 °C for 315 h and reported vacancy dislocation loops with $\boldsymbol{b} = \pm\frac{1}{2}\langle 111 \rangle$ type only. However, no dislocation analysis was reported pre-annealing and so it is not clear whether loops with $\boldsymbol{b} = \langle 100 \rangle$ were present prior to this. Rau et al. [16] also performed TEM analysis of fast-neutron irradiated Mo at 700 °C noting a dominance of $\boldsymbol{b} = \pm\frac{1}{2}\langle 111 \rangle$ and ~10% of $\boldsymbol{b} = \langle 100 \rangle$ type loops. The difference in the percentage of $\boldsymbol{b} = \langle 100 \rangle$ type loops in the neutron irradiated Mo (~10%) [16] and W self-ion irradiations (25% reported by Yi et al. [17,18] and 35–40% found in the current work) may be due to the differing PKA energies. The range of PKA energies in the fast neutron spectra from the work of Rau et al. [16] would have been 0.1–100 keV (from Ref. [29]) and in the self-ion irradiation work would have been 150 and 350 keV for Yi et al. [17,18] and the current work, respectively. The increasing PKA energies will result in a larger percentage of $\boldsymbol{b} = \langle 100 \rangle$ type loops being formed matching well with this trend in the reported experimental results [16–18] and results from MD simulations [19]. English and Jenkins [10] also report that the number density of $\boldsymbol{b} = \langle 100 \rangle$ type loops increased with both mass and energy in Mo irradiated with Sb, Sb_2 and

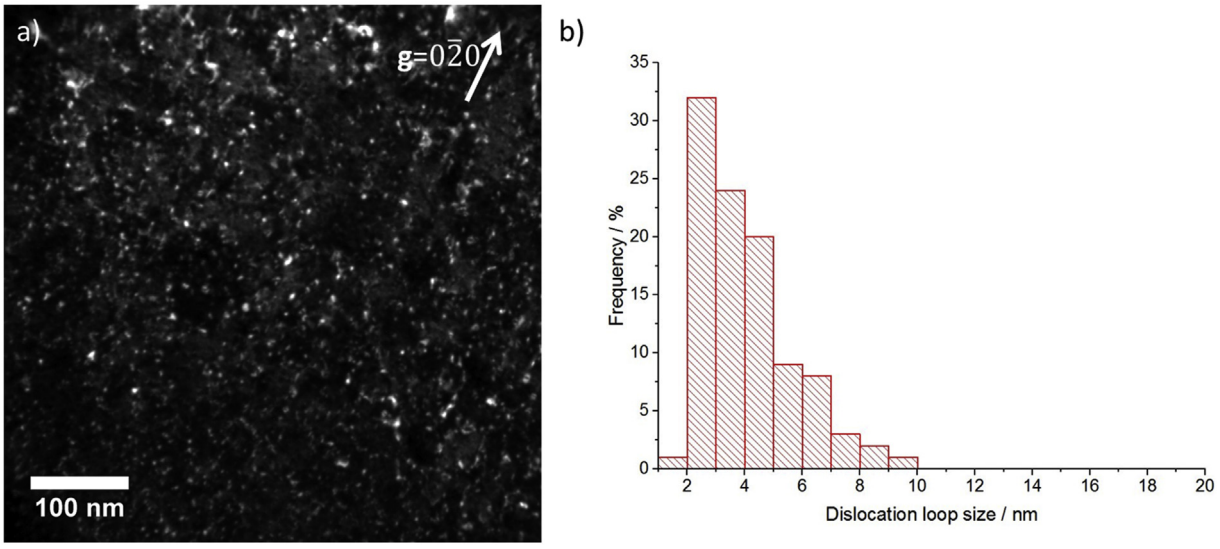

Fig. 4. a) WBDF image of W pre-implanted with 1500 appm He and then self-ion irradiated to a dose of 3.0 DPA at a temperature of 500 °C under (***g***,3***g***) conditions where $\boldsymbol{g} = (0\bar{2}0)$ and b) a histogram of dislocation loop sizes measured under these conditions.

Sb_3 molecular ions thus agreeing with the current work. This was attributed to the increased average energy density and thermal spike lifetime leading to an increased likelihood of the nucleated loop unfaulting to a $\boldsymbol{b} = \langle 100 \rangle$ type loop according to Eq. (2). However, Sand et al. [30] have used MD simulations to show that at PKA energies above 200 keV there is a greater likelihood of cascade fragmentation which would ultimately decrease the deposited-energy density. However, the authors also state that this is not a sharp transition and some cascades will still remain compact even at energies above which cascade splitting is observed.

These results demonstrate that there are significant consequences when considering PKA energy and mass on resulting cascade densities where the aim is to replicate neutron damage in W using ion beam(s). The increase in the percentage of $\boldsymbol{b} = \langle 100 \rangle$ type loops as a function of cascade size and density may also have implications for the mechanical degradation of the material. Dislocations with $\boldsymbol{b} = \langle 100 \rangle$ are generally much less mobile than those with $\boldsymbol{b} = \pm\frac{1}{2}\langle 111 \rangle$ for BCC materials [12,13,31] and would increase the radiation hardening and embrittlement.

Fig. 3a shows a WBDF image of a pristine W sample after irradiation and Fig. 3b shows a frequency distribution of loop sizes as measured from Fig. 3a for ~2–18 nm and with the largest frequency of loops at ~4–6 nm. Fig. 4a shows a WBDF image of W pre-implanted with 1500 appm He and self-ion irradiated to 3.0 DPA. Fig. 4b shows a frequency distribution of loop sizes as measured from Fig. 4a from ~2–10 nm with the largest frequency of loops at ~2–3 nm. This matches well with our previous work [2,3] where samples contained loops with sizes between 2.5 and 10 nm. At the temperature of 500 °C employed in these experiments, monointerstitials and interstitial clusters will be highly mobile [26,32–36] and monovacancy migration will also be active [35,37]. However, in the presence of He these defects may be less mobile as Gonzalez and Iglesias [38] reported the migration energy of a monovacancy increases from ~1.8 to 4.83 eV with the addition of a single He atom. The observation that the dislocation loop sizes are smaller in the case of the He pre-implantation shows that He may restrict the mobility of these mobile defects resulting in lower agglomeration and growth of defect clusters.

Dislocation loops with $\boldsymbol{b} = \pm\frac{1}{2}\langle 111 \rangle$ and $\boldsymbol{b} = \langle 100 \rangle$ were observed in both pristine W samples and those pre-implanted with He with similar percentages of $\boldsymbol{b} = \langle 100 \rangle$ loops in both cases. This is in contrast to the work that we have performed using only He ion irradiation where no $\boldsymbol{b} = \langle 100 \rangle$ type loops were observed. This shows that the energetically unfavourable $\boldsymbol{b} = \langle 100 \rangle$ dislocation loops form directly in dense cascades as predicated from MD simulations [39] and contrary to nucleation mechanisms of $\boldsymbol{b} = \langle 100 \rangle$ type loops in other BCC metals via reaction of $\boldsymbol{b} = \pm\frac{1}{2}\langle 111 \rangle$ type loops [12]. Pre-implantation does restrict dislocation loop growth and this is likely to be due to the pinning of mobile defects reducing absorption of migrating defects by larger dislocation loops. These results will have significant impact on the understanding of the mechanical degradation of these materials under irradiation and the considerations surrounding PKA energy and cascade size when the aim is to replicate neutron damage in W using ion beam(s).

Acknowledgments

The authors are grateful to the EPSRC for financial support of this project (EP/M011135/1 and EP/M028283/1).

References

[1] H. Bolt, V. Barabash, W. Krauss, J. Linke, R. Neu, S. Suzuki, N. Yoshida, A.U. Team, Materials for the Plasma-Facing Components of Fusion Reactors, 2004.
[2] R.W. Harrison, H. Amari, G. Greaves, J.A. Hinks, S.E. Donnelly, MRS Adv. 1 (2016) 2893–2899.
[3] R.W. Harrison, G. Greaves, J.A. Hinks, S.E. Donnelly, J. Nucl. Mater. 495 (2017) 492–503.
[4] T. Matsui, S. Muto, T. Tanabe, J. Nucl. Mater. 283–287 (2000) 1139–1143.
[5] I. Ipatova, P.T. Wady, S.M. Shubeita, C. Barcellini, A. Impagnatiello, E. Jimenez-Melero, J. Nucl. Mater. 495 (2017) 343–350.
[6] L. Fengfeng, W. Jiawei, G. Li-ping, Z. Linwei, S. Zhenyu, Z. Weiping, J. Wuhan, Univ. Nat. Sci. Ed. 8 (2017) 349–354.
[7] B.L. Eyre, R. Bullough, Philos. Mag. A J. Theor. Exp. Appl. Phys. 12 (1965) 31–39.
[8] D. Nguyen-Manh, A.P. Horsfield, S.L. Dudarev, Phys. Rev. B 73 (2006) 20101.
[9] D. Nguyen-Manh, S.L. Dudarev, A.P. Horsfield, J. Nucl. Mater. 367–370A (2007) 257–262.
[10] C.A. English, M.L. Jenkins, Philos. Mag. 90 (2010) 821–843.
[11] W. Jäger, M. Wilkens, Phys. Status Solidi 32 (1975) 89–100.
[12] A. Prokhodtseva, B. Décamps, A. Ramar, R. Schäublin, Acta Mater. 61 (2013) 6958–6971.
[13] H. Xu, R.E. Stoller, Y.N. Osetsky, D. Terentyev, Phys. Rev. Lett. 110 (2013).
[14] B.C. Masters, Philos. Mag. A J. Theor. Exp. Appl. Phys. 11 (1965) 881–893.
[15] R. Schäublin, B. Décamps, A. Prokhodtseva, J.F. Löffler, Acta Mater. 133 (2017) 427–439.
[16] R.C. Rau, F.S. D'Aragona, R.L. Ladd, Philos. Mag. A J. Theor. Exp. Appl. Phys. 21 (1970) 441–452.
[17] X. Yi, M.L. Jenkins, M. Briceno, S.G. Roberts, Z. Zhou, Philos. Mag. A 93 (2013) 1715–1738.
[18] X. Yi, M.L. Jenkins, M.A. Kirk, Z. Zhou, S.G. Roberts, Acta Mater. 112 (2016) 105–120.
[19] A.E. Sand, S.L. Dudarev, K. Nordlund, EPL (Europhys. Lett.) 103 (2013) 46003.
[20] J.F. Ziegler, J. Appl. Phys. 85 (1999) 1249.
[21] R.E. Stoller, M.B. Toloczko, G.S. Was, A.G. Certain, S. Dwaraknath, F.A. Garner, Nucl. Instruments Methods Phys. Res. Sect. B Beam Interact. Mater. Atoms 310 (2013) 75–80.
[22] G.S. Was, Fundamentals of Radiation Materials Science, 1st ed. Springer-Verlag, Berlin Heidelberg, New York, 2007.
[23] A. Hasegawa, M. Fukuda, K. Yabuuchi, S. Nogami, J. Nucl. Mater. 471 (2016) 175–183.
[24] T. Koyanagi, N.A.P.K. Kumar, T. Hwang, L.M. Garrison, X. Hu, L.L. Snead, Y. Katoh, J. Nucl. Mater. 490 (2017) 66–74.
[25] X. Hu, T. Koyanagi, M. Fukuda, N.A.P.K. Kumar, L.L. Snead, B.D. Wirth, Y. Katoh, J. Nucl. Mater. 480 (2016) 235–243.
[26] T. Tanno, A. Hasegawa, J.C. He, M. Fujiwara, M. Satou, S. Nogami, K. Abe, T. Shishido, J. Nucl. Mater. 386–388 (2009) 218–221.
[27] T. Tanno, A. Hasegawa, J.-C. He, M. Fujiwara, S. Nogami, M. Satou, T. Shishido, K. Abe, Mater. Trans. 48 (2007) 2399–2402.
[28] R.C. Rau, Philos. Mag. A J. Theor. Exp. Appl. Phys. 18 (1968) 1079–1084.
[29] R. Mark, J.-C. Gilbert, Sublet, Handbook of Activation, Transmutation, and Radiation Damage Properties of the Elements Simulated Using FISPACT-II & TENDL-2014; Nuclear Fission Plants (FBR Focus) UKAEA-R(15)33, 2015.
[30] A.E. Sand, D.R. Mason, A. De Backer, X. Yi, S.L. Dudarev, K. Nordlund, Mater. Res. Lett. 5 (2017) 357–363.
[31] X. Yi, M.L. Jenkins, K. Hattar, P.D. Edmondson, S.G. Roberts, Acta Mater. 92 (2015) 163–177.
[32] A. Hasegawa, M. Fukuda, S. Nogami, K. Yabuuchi, Fusion Eng. Des. 89 (2014) 1568–1572.
[33] F. Maury, M. Biget, P. Vajda, A. Lucasson, P. Lucasson, Radiat. Eff. Inc. Plasma Sci. Plasma Technol. 38 (1978) 1–2.
[34] R.W. Balluffi, J. Nucl. Mater. 69–70 (1978) 240–263.
[35] F. Ferroni, X. Yi, K. Arakawa, S.P. Fitzgerald, P.D. Edmondson, S.G. Roberts, Acta Mater. 90 (2015) 380–393.
[36] D.R. Mason, X. Yi, M.A. Kirk, S.L. Dudarev, J. Phys. Condens. Matter 26 (2014) 1–28.
[37] O. El-Atwani, J.A. Hinks, G. Greaves, S. Gonderman, T. Qiu, M. Efe, J.P. Allain, Sci. Rep. 4 (2015) 4716.
[38] C. González, R. Iglesias, J. Mater. Sci. 49 (2014) 8127–8139.
[39] A.E. Sand, K. Nordlund, S.L. Dudarev, J. Nucl. Mater. 455 (2014) 207–211.